PERGAMON

International Journal of Solids and Structures 38 (2001) 5935–5947

INTERNATIONAL JOURNAL OF SOLIDS and STRUCTURES

www.elsevier.com/locate/ijsolstr

Development of a three-dimensional mixed variational model for woven composites. I. Mathematical formulation

Ajit K. Roy [a,*], Sangwook Sihn [b]

[a] *Air Force Research Laboratory, Materials and Manufacturing Directorate, AFRL/MLBC, 2941 P St Rm. 136, WPAFB, OH 45433-7750, USA*

[b] *University of Dayton Research Institute, 300 College Park Avenue, Dayton, OH 45469-0168, USA*

Received 23 March 2000

Abstract

A mixed three-dimensional variational model has been derived for stress analysis of a representative volume element of woven fabric composites, based on the Reissner variational principle. In this model, each yarn is modeled as a homogeneous orthotropic (in its own material axes) medium, and the matrix regions that exist around the wavy yarns are also represented as separate regions in the model. In order to accurately predict the characteristic damage (crack initiation and its propagation), the equilibrium of stresses is satisfied pointwise everywhere in the model, and the yarn-interface stress compatibility is enforced in the model. The variational principle yields a set of second-order partial differential equations, which can numerically be solved by either by finite element or finite difference approaches. A solution procedure with representative results is given in an adjoining paper. © 2001 Elsevier Science Ltd. All rights reserved.

Keywords: Woven composite; Fabric composite; Reissner variational principle; Three-dimensional stress analysis

1. Introduction

The woven fabric (textile) composite is widely used in advanced composite manufacturing and key to many affordable composite parts of complex shapes. The performance of such structures is ultimately influenced by the deformation characteristics and failure mechanism of woven composites. Further, to achieve the optimum structural properties of these parts, there is a need to develop a basic understanding of deformation/damage mechanics and failure mechanisms of textile composites. The in situ experimental observation of damage initiation in woven composites reveals that the damage initiates in the form of interface cracks in the vicinity of yarn crimping, Roy (1996, 1998), which is strongly influenced by the interlaminar stresses at a location of significant strain gradients, Fig. 1. At the yarn crimping location, fiber tows (or yarns) are intertwined with each other in perpendicular direction (Fig. 2). Due to the perpendicular

* Corresponding author. Tel.: +1-937-255-9034; fax: +1-937-656-4706.
E-mail address: ajit.roy@wpafb.af.mil (A.K. Roy).

0020-7683/01/$ - see front matter © 2001 Elsevier Science Ltd. All rights reserved.
PII: S0020-7683(00)00404-2

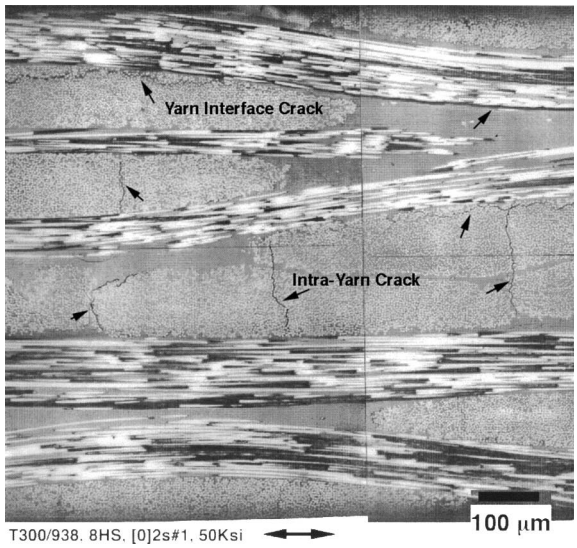

Fig. 1. A representative cross-sectional micrograph of an 8HS woven T300/938 (graphite/epoxy) composite at 70% of the failure load.

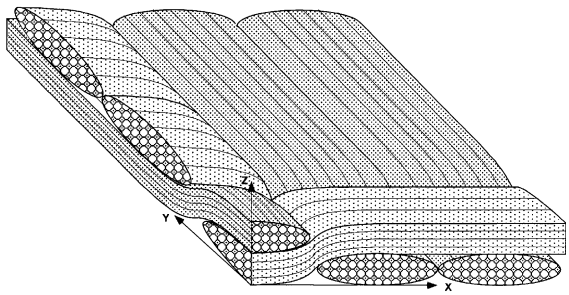

Fig. 2. The RVE of a 2D woven composite.

yarn crimping, even under the application of simple unidirectional load, the stresses in the vicinity of the yarn crimping are three-dimensional, Whitcomb (1991). Thus an accurate prediction of the interlaminar stresses at the interface region is needed to reliably analyze damage initiation and propagation in woven composites. Most of the research work in this area, however, is based on two-dimensional stress analysis, Naik and Ganesh (1994), Karayaka and Kurath (1994), which does not reliably predict the interlaminar stresses. Further, traditional finite-element analysis only predicts stresses accurate at the Gaussian integration points (interior to the element boundary), and stresses are derived from the displacement field at the element level. Thus, traditional displacement-based finite element analysis is not expected to yield interface stress continuity in the vicinity of yarn crimping location, as observed by Marrey and Sankar (1995).

The analytical model developed in this work is based on the Reissner mixed variational principle, Reissner (1950), where the variations of both stresses and displacement are performed to obtain reliable interface stress continuity. Pagano (1978) applied Reissner variational principle analyzing stress field in flat composite, and recently Harrison and Johnson (1996) applied the same principle analyzing stress field in tapered laminates. The Pagano's composite laminate problem contained flat (no curvature) interface, and Harrison and Johnson dealt with material interface containing one-dimensional curvature. In the present

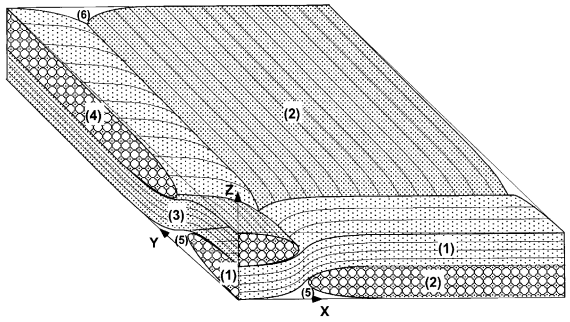

Fig. 3. RVE of the analytical model.

model, however, due to the weaving architecture, the representative volume element (RVE) contains two-dimensionally curved material interfaces intersecting at the yarn intertwining location (Fig. 2). In this model, as was utilized by Pagano (1978), and Harrison and Johnson (1996), the continuity of both tractions and displacements is imposed at the yarn (material) interface. Further, the equilibrium of stresses is satisfied pointwise and the variational principle yields energy both in stresses and displacements; an accurate prediction of stress field is thus expected with this model. The RVE of the model is divided into several subregions; a characteristic fabric yarn or matrix region (Fig. 3) occupies each subregion. The mathematical derivation of the governing equations and the interface continuity conditions of the subregions (yarns) of the RVE are derived in this paper. The governing and interface continuity conditions are a set of partial differential equations. The solution for this set of partial differential equations can be numerically obtained either by a finite element or a finite difference scheme. The numerical solution and validation of the mathematical formulation is presented in Part II, an adjoining paper.

2. Model geometry

The RVE of woven composite contains all the characteristic yarns and the matrix region to represent a repeating unit cell of the weaving pattern, and the geometry of the RVE changes with the weaving pattern (such as plain weave (PW), 5HS, 8HS, etc.). The RVE of a few of these weaving patterns is schematically shown in Chou and Ko (1989). In order to obtain a good accuracy in the stress field, the RVE is subdivided in several subregions representing the characteristic yarns and the matrix regions. In PW architecture the adjacent yarns are alternately cross-crimping with its perpendicular yarns. Thus PW does not contain adjacent yarns of self-similar weaving patterns. Other weaving architectures, such as 5HS and 8HS, contain adjacent self-similar weaving yarns. Fig. 2 shows two such yarns of self-similar pattern both in x and y directions, next to the intertwined cross-crimped yarns. The cross-sectional micrograph of woven composites (as can be seen in Fig. 1 of an 8HS composite) reveals that the self-similar weaving yarns are packed together during the fabrication process. Thus, in view of keeping the size of the computational problem to a reasonable level, it is viewed acceptable that the yarns of self-similar weaving (crimping) pattern be lumped in one subregion, as illustrated in Fig. 3. In Fig. 3, subregions 2 and 4 represent the self-similar yarns aligned along y (fill) and x (warp) directions, respectively. Thus, in the absence of any damage (cracks), the RVE contains six subregions, see Fig. 3. Among the six subregions in Fig. 3, two are associated with yarns aligned in warp direction (subregions 1 and 4), two subregions (subregions 2 and 3) are for fill yarns, and subregions 5 and 6 are associated with lower and upper matrix regions near the crimp location, respectively. As we introduce cracks in the RVE, to study fracture toughness and energy release rates, etc., the number of subregions in the RVE will increase accordingly. The geometry of each subregion is defined by two of its

boundary surfaces; lower boundary (h_1) and upper boundary (h_2). Due to yarn waviness and nonrectangular cross-section of the yarns, h_1 and h_2 are functions of both x and y. The in situ observation of crimped composites revealed that the crimp angle practically remained unchanged during loading (Roy, 1996, 1998). Thus geometric nonlinearity is not included in this study.

Since each subregion is configured to contain a characteristic yarn or matrix region, the materials in subregions containing yarns are modeled as transversely isotropic (or isotropic for matrix regions) homogeneous materials with the major material symmetry axis aligned parallel to yarn fiber axis. Due to yarn crimping, the material properties of the subregions containing yarns, when transformed to RVE coordinate system (x, y, z) possess monoclinic material symmetry. It is generally known that the material nonlinearity (especially the shear component) influences the stress field on off-axis composites (presence of off-axis is due to yarn crimping). However, in view of the crimp (off-axis) angle in woven composites being very small (in the order of 4–5° or 0.07–0.09 rad), the material nonlinearity is not considered in this study.

3. Variational formulation of the model

Besides analyzing the stress field of undamaged woven composite system, a long-term objective is to use this model to study fracture toughness (energy release rates, etc.) of woven composites. Thus, for an accurate prediction of energy release rates, etc., continuity conditions (stresses and displacements) at the interface need to be satisfied as accurately as possible. In the vicinity of a cracked interface (location of high strain gradient), the stress continuity condition is difficult to be satisfied with traditional displacement based finite element method. Thus, the present model is derived from the Reissner variational principle (a mixed variational principle), where the variation of the stresses is taken independent of that of the displacement field. The governing equations of elasticity in terms of the Cartesian coordinates, (x, y, z), can be obtained from the following variational equation developed by Reissner (1950)

$$\delta J = 0 \tag{1}$$

where

$$J = \int_v F \, \mathrm{d}V - \int_{\Gamma_\tau} \tilde{\tau}_i u_i \, \mathrm{d}\Gamma \tag{2}$$

and

$$F = \tfrac{1}{2}\sigma_{ij}\left(u_{i,j} + u_{j,i}\right) - W(\sigma_i, e_i) \tag{3}$$

In these equations, W is the strain energy density expressed in terms of the stresses σ_{ij}; V is the volume; Γ the entire surface; $\tilde{\tau}_i$ the prescribed tractions; u_i the displacement components; and Γ_τ is the portion of the boundary on which one or more traction components are prescribed. It is understood that both stresses and displacements are subjected to variation in the application of Eq. (1), and summation over the range of repeated subscripts (but not superscripts) is implied throughout the work.

As described above, each subregion containing yarns is modeled as homogeneous medium with monoclinic material symmetry with respect to the RVE coordinate. In order to derive the governing equations from Eqs. (1)–(3), we need to first define stress field for each subregion. Contracted notation is employed in the representation of the stress and strain components, i.e.,

$$\sigma_1 = \sigma_x, \quad \sigma_2 = \sigma_y, \quad \sigma_3 = \sigma_z, \quad \sigma_4 = \sigma_{yz}, \quad \sigma_5 = \sigma_{xz}, \quad \sigma_6 = \sigma_{xy} \tag{4}$$

and analogous relation for the engineering strain components, e_i $(i = 1, \ldots, 6)$.

The average yarn waviness ratio (ratio of the waviness amplitude to the length of the wave) of a typical 12K tow 8HS woven fabric composites due to yarn crimping is about 0.05 (Roy, 1996). With an average yarn thickness of 0.125 mm in such fabric, the value of the radius of curvature to thickness ratio (R/t)

around the crimped location results in to be about 25. For such a value of R/t ratio, the weaving curvature effect on the through-the-thickness stress distribution within a yarn is assumed negligible. Further, the ratio of the in-plane dimension of the RVE to yarn thickness varies typically around 15 (for PW) to 60 (for 8HS), which implies that the yarn (subregion) can be considered thin compared to the in-plane dimension of the RVE. Thus it is reasonable to assume that the in plane stresses, within a subregion (yarn), to vary linearly through the thickness. Then, the expression for the out-of-plane stresses are obtained by satisfying the equations of equilibrium to ensure the equilibrium of stresses pointwise. The expressions of the stress components are as follows

$$\sigma_i = p_{iK} f_K^{(i)} \quad (i = 1\text{–}6,\ K = 1\text{–}4) \tag{5}$$

where p_{iK} are functions of x and y and $f_K^{(i)}$ are functions of z only. The functions $f_K^{(i)}$ $(K = 1, 2)$ associated with the in-plane stresses, as discussed above, are linear functions of z, and $f_K^{(i)}$ $(K = 3, 4)$ associated with the interlaminar stresses, derived by satisfying the linear elasticity equations of equilibrium and are higher order polynomials. The expressions for $f_K^{(i)}$ are as follows

$$f_1^{(1)} = f_1^{(2)} = f_1^{(3)} = f_1^{(4)} = f_1^{(5)} = f_1^{(6)} = \frac{h_2 - z}{h_2 - h_1} \tag{6}$$

$$f_2^{(1)} = f_2^{(2)} = f_2^{(3)} = f_2^{(4)} = f_2^{(5)} = f_2^{(6)} = \frac{z - h_1}{h_2 - h_1} \tag{7}$$

$$f_3^{(3)} = f_3^{(4)} = f_3^{(5)} = \frac{z^2 - z(h_1 + h_2) + h_1 h_2}{(h_2 - h_1)^2} \tag{8}$$

$$f_4^{(3)} = \frac{2z^3 - 3z^2(z_1 + z_2) + z(h_1^2 + 4h_1 h_2 + h_2^2) - h_1 h_2 (h_1 + h_2)}{(h_2 - h_1)^3} \tag{9}$$

with

$$f_K^{(i)} = 0 \quad (i = 1, 2, 6 \text{ and } K = 3, 4; i = 4, 5 \text{ and } K = 4) \tag{10}$$

The expressions of the stresses are substituted in Eqs. (2) and (3) to derive the governing equations. The strain energy density, W in Eq. (3), of a subregion (an elastic body of monoclinic material symmetry), including the influence of free expansion, is given by

$$W = \tfrac{1}{2} S_{ij} \sigma_i \sigma_j + \sigma_i e_i \tag{11}$$

where S_{ij} is the elements of the compliance matrix of monoclinic material symmetry, and e_i is the strain due to free expansion.

In order to reduce the size of the numerical problem, after substituting the expression of stresses in Eq. (2), the integration with respect to thickness (z) is performed. The integration with respect to z also gives rise to weighted average displacements and the displacements on the surfaces $z = h_1$, h_2. The definitions of the weighted displacements are (q may represent either u, v, or w)

$$[\bar{q}(x, y), q^*(x, y), \hat{q}(x, y)] = \int_{h_1}^{h_2} [H_1, H_2, H_3] q(x, y, z)\, \mathrm{d}z \tag{12}$$

where

$$H_1 = \frac{h_2 - z}{(h_2 - h_1)^2}, \qquad H_2 = \frac{z - h_1}{(h_2 - h_1)^2}, \qquad H_3 = \frac{z^2 - z(h_1 + h_2) - h_1 h_2}{(h_2 - h_1)^3}$$

Further, because of the dependence of the subregion surface boundaries (h_1 and h_2) on x and y, Leibnitz's theorem in the following form must be applied in Eq. (2) on terms involving derivatives in x and y.

$$\int_{h_1(x,y)}^{h_2(x,y)} \frac{\partial}{\partial\xi} G(x,y,z)\,\mathrm{d}z = \frac{\mathrm{d}}{\mathrm{d}\xi}\int_{h_1(x,y)}^{h_2(x,y)} G(x,y,z)\,\mathrm{d}z - \frac{\partial h_2}{\partial\xi} G(x,y,h_2) + \frac{\partial h_1}{\partial\xi} G(x,y,h_1) \tag{13}$$

where ξ represents either x or y, and G is a general function of x, y, and z.

After substituting Eqs. (3)–(12) into Eq. (2), and using Eq. (13) where appropriate we obtain

$$\begin{aligned}
J = {} & \int\int_{xy} \sum_{k=1}^{N} \left[(\mu_{iJ} + \chi_{iJ})^{(k)} p_{iJ}^{(k)} - (F_1\bar{u} + F_2 u^* + F_3\bar{v} + F_4 v^* + F_5\bar{w} + F_6 w^* + F_7\hat{w})^{(k)} \right] \mathrm{d}x\,\mathrm{d}y \\
& + \int\int_{xy} \sum_{k=1}^{N} \Big[\left(p_{52}^{(k)} - h_{2,x}^{(k)} p_{12}^{(k)} - h_{2,y}^{(k)} p_{62}^{(k)} \right) u_2^{(k)} + \left(h_{1,x}^{(k)} p_{11}^{(k)} + h_{1,y}^{(k)} p_{61}^{(k)} - p_{51}^{(k)} \right) u_1^{(k)} \\
& \qquad + \left(p_{42}^{(k)} - h_{2,x}^{(k)} p_{62}^{(k)} - h_{2,y}^{(k)} p_{22}^{(k)} \right) v_2^{(k)} + \left(h_{1,x}^{(k)} p_{61}^{(k)} + h_{1,y}^{(k)} p_{21}^{(k)} - p_{41}^{(k)} \right) v_1^{(k)} + \left(p_{32}^{(k)} - h_{2,x}^{(k)} p_{52}^{(k)} - h_{2,y}^{(k)} p_{42}^{(k)} \right) w_2^{(k)} \\
& \qquad + \left(h_{1,x}^{(k)} p_{51}^{(k)} + h_{1,y}^{(k)} p_{41}^{(k)} - p_{31}^{(k)} \right) w_1^{(k)} \Big] \mathrm{d}x\,\mathrm{d}y \\
& + \int_x \sum_{k=1}^{N} \left\{ \left[p_{61}^{(k)}\bar{u}^{(k)} + p_{62}^{(k)} u^{*(k)} + p_{21}^{(k)}\bar{v}^{(k)} + p_{22}^{(k)} v^{*(k)} + p_{41}^{(k)}\bar{w}^{(k)} + p_{42}^{(k)} w^{*(k)} + p_{43}^{(k)}\hat{w}^{(k)} \right] \left(h_2^{(k)} - h_1^{(k)} \right) \right\}_{y_1}^{y_2} \mathrm{d}x \\
& + \int_y \sum_{k=1}^{N} \left\{ \left[p_{11}^{(k)}\bar{u}^{(k)} + p_{12}^{(k)} u^{*(k)} + p_{61}^{(k)}\bar{v}^{(k)} + p_{62}^{(k)} v^{*(k)} + p_{51}^{(k)}\bar{w}^{(k)} + p_{52}^{(k)} w^{*(k)} + p_{53}^{(k)}\hat{w}^{(k)} \right] \left(h_2^{(k)} - h_1^{(k)} \right) \right\}_{x_1}^{x_2} \mathrm{d}y \\
& - \int_\Gamma \left[\left(\tilde{\tau}_{x2} u_2 + \tilde{\tau}_{y2} v_2 + \tilde{\tau}_{z2} w_2 \right) - \left(\tilde{\tau}_{x1} u_1 + \tilde{\tau}_{y1} v_1 + \tilde{\tau}_{z1} w_1 \right) \right] \mathrm{d}\Gamma
\end{aligned} \tag{14}$$

where μ_{ij} and χ_{ij} are defined in Appendix A. The superscript k in the above equation represents a subregion. However, superscript k and l appeared later equation (17) represent the lower and upper subregions, respectively, sharing a common interface. The subscript ',' represents the partial derivative of a variable with respect to x or y. The variables containing subscripts 1 and 2 in the above equation are associated with the lower and upper surface of a subregion, respectively. For example, $u_1^{(k)}$ and $u_2^{(k)}$ represent the u displacement at lower and upper surface of subregion k, respectively.

There are $29N$ unknown variables (N being the total number of subregions) in Eq. (14) to be determined. All terms in Eq. (14) are not independent. Now we need to impose the interface (traction and displacement) continuity condition of the subregions to determine the independent terms that are necessary to determine $29N$ unknown variables. The interface tractions are obtained by defining the unit vectors $(\hat{t}, \hat{s}, \hat{n})$ associated with the interface surface, where $\hat{n}$ is the normal vector and $\hat{t}$ and $\hat{s}$ two surface vectors (see Fig. 4). For

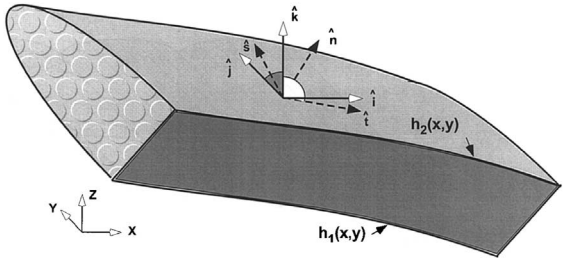

Fig. 4. The configuration of the normal (n) and tangential (t, s) vectors on an interface.

convenience, the surface vector $\hat{t}$ is defined being in the plane containing $\hat{i}$ and $\hat{k}$, and $\hat{s}$ being in the plane containing $\hat{j}$ and $\hat{k}$. The interface surface unit vectors $(\hat{t},\hat{s},\hat{n})$ expressed with respect to the unit vectors ($\hat{i},\hat{j}$, and $\hat{k}$) associated with the RVE coordinate system (x,y,z) as follows.

$$\begin{Bmatrix} \hat{t} \\ \hat{s} \\ \hat{n} \end{Bmatrix} = \begin{bmatrix} a_{11} & a_{12} & a_{13} \\ a_{21} & a_{22} & a_{23} \\ a_{31} & a_{32} & a_{33} \end{bmatrix} \begin{Bmatrix} \hat{i} \\ \hat{j} \\ \hat{k} \end{Bmatrix} \tag{15}$$

where a_{ij} are the direction cosines. The direction cosines a_{ij} are also used for transforming stresses between the two coordinate systems, $(\hat{t},\hat{s},\hat{n})$ and $(\hat{i},\hat{j},\hat{k})$. The direction cosines a_{ij} obtained in terms of surface slopes are given in Table 1. The interface displacement continuity condition between two adjacent subregions, l (upper subregion) and k (lower subregion) is a trivial one ($u_1^{(l)} = u_2^{(k)}, v_1^{(l)} = v_2^{(k)}, w_1^{(l)} = w_2^{(k)}$). The interface traction continuity condition ($\hat{\sigma}_4^{(l)} = \hat{\sigma}_4^{(k)}, \hat{\sigma}_5^{(l)} = \hat{\sigma}_5^{(k)}, \hat{\sigma}_3^{(l)} = \hat{\sigma}_3^{(k)}$), after transforming the surface tractions to $(\hat{i},\hat{j},\hat{k})$ or (x,y,z) coordinate system, becomes

$$\begin{Bmatrix} p_{31}^{(l)} - p_{32}^{(k)} \\ p_{41}^{(l)} - p_{42}^{(k)} \\ p_{51}^{(l)} - p_{52}^{(k)} \end{Bmatrix} = \begin{bmatrix} \left(h_{2,x}^{(k)}\right)^2 & \left(h_{2,y}^{(k)}\right)^2 & 2h_{2,x}^{(k)}h_{2,y}^{(k)} \\ 0 & h_{2,y}^{(k)} & h_{2,x}^{(k)} \\ h_{2,x}^{(k)} & 0 & h_{2,y}^{(k)} \end{bmatrix} \begin{Bmatrix} p_{11}^{(l)} - p_{12}^{(k)} \\ p_{21}^{(l)} - p_{22}^{(k)} \\ p_{61}^{(l)} - p_{62}^{(k)} \end{Bmatrix} \tag{16}$$

After applying the above interface displacement and traction continuity conditions in Eq. (14) and taking its first variation we obtain

$$\begin{aligned}
\delta J = & \int\int_{xy} \sum_{k=1}^{N} \left[\chi_{33}^{(k)} \delta p_{33}^{(k)} + \chi_{34}^{(k)} \delta p_{34}^{(k)} + \chi_{43}^{(k)} \delta p_{43}^{(k)} + \chi_{53}^{(k)} \delta p_{53}^{(k)} \right] \mathrm{d}x\,\mathrm{d}y \\
& - \int\int_{xy} \sum_{k=1}^{N} \left[\left(F_1 \delta \bar{u} + F_2 \delta u^* + F_3 \delta \bar{v} + F_4 \delta v^* + F_5 \delta \bar{w} + F_6 \delta w^* + F_7 \delta \hat{w} \right)^{(k)} \right] \mathrm{d}x\,\mathrm{d}y \\
& + \int\int_{xy} \sum_{k=1}^{N-1} \Big[\left(\chi_{11}^{(l)} + \chi_{12}^{(k)} \right) \delta p_{11}^{(l)} + \left(\chi_{21}^{(l)} + \chi_{22}^{(k)} \right) \delta p_{21}^{(l)} + \left(\chi_{31}^{(l)} + \chi_{32}^{(k)} \right) \delta p_{31}^{(l)} + \left(\chi_{41}^{(l)} + \chi_{42}^{(k)} \right) \delta p_{41}^{(l)} + \left(\chi_{51}^{(l)} + \chi_{52}^{(k)} \right) \delta p_{51}^{(l)} \\
& \quad + \left(\chi_{61}^{(l)} + \chi_{62}^{(k)} \right) \delta p_{61}^{(l)} + \left(\chi_{12}^{(k)} + h_{2,x}^{(k)} \chi_{52}^{(k)} + \left(h_{2,x}^{(k)} \right)^2 \chi_{32}^{(k)} \right) \delta p_{12}^{(k)} + \left(\chi_{22}^{(k)} + h_{2,y}^{(k)} \chi_{42}^{(k)} + \left(h_{2,y}^{(k)} \right)^2 \chi_{32}^{(k)} \right) \delta p_{22}^{(k)} \\
& \quad + \left(\chi_{62}^{(k)} + h_{2,x}^{(k)} \chi_{42}^{(k)} + h_{2,y}^{(k)} \chi_{52}^{(k)} + 2h_{2,x}^{(k)} h_{2,y}^{(k)} \chi_{32}^{(k)} \right) \delta p_{62}^{(k)} + \left(p_{52}^{(k)} - h_{2,x}^{(k)} p_{12}^{(k)} - h_{2,y}^{(k)} p_{62}^{(k)} + h_{2,x}^{(k)} p_{11}^{(l)} \right. \\
& \quad \left. + h_{2,y}^{(k)} p_{61}^{(l)} - p_{51}^{(l)} \right) u_2^{(k)} + \left(p_{42}^{(k)} - h_{2,x}^{(k)} p_{62}^{(k)} - h_{2,y}^{(k)} p_{22}^{(k)} + h_{2,x}^{(k)} p_{61}^{(l)} + h_{2,y}^{(k)} p_{21}^{(l)} - p_{41}^{(l)} \right) v_2^{(k)} \\
& \quad + \left(p_{32}^{(k)} - h_{2,x}^{(k)} p_{52}^{(k)} - h_{2,y}^{(k)} p_{42}^{(k)} + h_{2,x}^{(k)} p_{51}^{(l)} + h_{2,y}^{(k)} p_{41}^{(l)} - p_{31}^{(l)} \right) w_2^{(k)} \Big] \mathrm{d}x\,\mathrm{d}y \\
& + \int\int_{xy} \Big[\left(\chi_{11}^{(m)} + h_{1,x}^{(m)} \chi_{51}^{(m)} + \left(h_{1,x}^{(m)} \right)^2 \chi_{31}^{(m)} \right) \delta p_{11}^{(m)} + \left(\chi_{21}^{(m)} + h_{1,y}^{(m)} \chi_{41}^{(m)} + \left(h_{1,y}^{(m)} \right)^2 \chi_{31}^{(m)} \right) \delta p_{21}^{(m)} \\
& \quad + \left(\chi_{61}^{(m)} + h_{1,x}^{(m)} \chi_{41}^{(m)} + h_{1,y}^{(m)} \chi_{51}^{(m)} + 2h_{1,x}^{(m)} h_{1,y}^{(m)} \chi_{31}^{(m)} \right) \delta p_{61}^{(m)} + \left(\chi_{12}^{(n)} + h_{2,x}^{(n)} \chi_{52}^{(n)} + \left(h_{2,x}^{(n)} \right)^2 \chi_{32}^{(n)} \right) \delta p_{12}^{(n)} \\
& \quad + \left(\chi_{22}^{(n)} + h_{2,y}^{(n)} \chi_{42}^{(n)} + \left(h_{2,y}^{(n)} \right)^2 \chi_{32}^{(n)} \right) \delta p_{22}^{(n)} + \left(\chi_{62}^{(n)} + h_{2,x}^{(n)} \chi_{42}^{(n)} + h_{2,y}^{(n)} \chi_{52}^{(n)} \right. \\
& \quad \left. + 2h_{2,x}^{(n)} h_{2,y}^{(n)} \chi_{32}^{(n)} \right) \delta p_{62}^{(n)} \Big] \mathrm{d}x\,\mathrm{d}y + \delta J_\Gamma = 0
\end{aligned} \tag{17}$$

where, if displacements are prescribed at the boundary

Table 1
Direction cosines of the interface surface vectors

	$\hat{i}$	$\hat{j}$	$\hat{k}$
$\hat{t}$	$a_{11}=\frac{1}{\sqrt{1+(h_{,x})^2}}$	$a_{12}=0$	$a_{13}=\frac{h_{,x}}{\sqrt{1+(h_{,x})^2}}$
$\hat{s}$	$a_{21}=0$	$a_{22}=\frac{1}{\sqrt{1+(h_{,y})^2}}$	$a_{23}=\frac{h_{,y}}{\sqrt{1+(h_{,y})^2}}$
$\hat{n}$	$a_{31}=-\frac{a_{22}a_{13}}{\sqrt{1-a_{13}a_{23}}}$	$a_{32}=-\frac{a_{11}a_{23}}{\sqrt{1-a_{13}a_{23}}}$	$a_{33}=\frac{a_{11}a_{22}}{\sqrt{1-a_{13}a_{23}}}$

$$\delta J_\Gamma=\int\int_{xy}\Big[\Big(\chi_{52}^{(n)}+h_{2,x}^{(n)}\chi_{52}^{(n)}+\tilde{u}_2^{(n)}\Big)\delta p_{52}^{(n)}+\Big(\chi_{42}^{(n)}+h_{2,y}^{(n)}\chi_{32}^{(n)}+\tilde{v}_2^{(n)}\Big)\delta p_{42}^{(n)}+\Big(\chi_{32}^{(n)}+\tilde{w}_2^{(n)}\Big)\delta p_{32}^{(n)}$$
$$-\Big(\chi_{51}^{(m)}+h_{1,x}^{(m)}\chi_{51}^{(m)}+\tilde{u}_1^{(m)}\Big)\delta p_{51}^{(m)}-\Big(\chi_{41}^{(m)}+h_{1,y}^{(m)}\chi_{31}^{(m)}+\tilde{v}_1^{(m)}\Big)\delta p_{41}^{(m)}-\Big(\chi_{31}^{(m)}+\tilde{w}_1^{(m)}\Big)\delta p_{31}^{(m)}\Big]\,\mathrm{d}x\,\mathrm{d}y \tag{18}$$

and, if tractions are prescribed at the boundary

$$\begin{aligned}\delta J_\Gamma=\int\int_{xy}\Big[&\Big(\cos\alpha_n\cos\beta_n p_{52}^{(n)}-\sin\alpha_n\cos\beta_n p_{12}^{(n)}-\cos\alpha_n\sin\beta_n p_{62}^{(n)}-\tau_{x2}^{(n)}\Big)\delta u_2^{(n)}\\&+\Big(\cos\alpha_n\cos\beta_n p_{42}^{(n)}-\sin\alpha_n\cos\beta_n p_{62}^{(n)}-\cos\alpha_n\sin\beta_n p_{22}^{(n)}-\tau_{y2}^{(n)}\Big)\delta v_2^{(n)}\\&+\Big(\cos\alpha_n\cos\beta_n p_{32}^{(n)}-\sin\alpha_n\cos\beta_n p_{52}^{(n)}-\cos\alpha_n\sin\beta_n p_{42}^{(n)}-\tau_{z2}^{(n)}\Big)\delta w_2^{(n)}\\&-\Big(\cos\alpha_m\cos\beta_m p_{51}^{(m)}-\sin\alpha_m\cos\beta_m p_{11}^{(m)}-\cos\alpha_m\sin\beta_m p_{61}^{(m)}-\tau_{x1}^{(m)}\Big)\delta u_1^{(m)}\\&-\Big(\cos\alpha_m\cos\beta_m p_{41}^{(m)}-\sin\alpha_m\cos\beta_m p_{61}^{(m)}-\cos\alpha_m\sin\beta_m p_{21}^{(m)}-\tau_{y1}^{(m)}\Big)\delta v_1^{(m)}\\&-\Big(\cos\alpha_m\cos\beta_m p_{31}^{(m)}-\sin\alpha_m\cos\beta_m p_{51}^{(m)}-\cos\alpha_m\sin\beta_m p_{41}^{(m)}-\tau_{z1}^{(m)}\Big)\delta w_1^{(m)}\Big]\,\mathrm{d}x\,\mathrm{d}y\end{aligned} \tag{19}$$

The subscripts or superscripts m and n are associated with the bottom and top surfaces of the RVE respectively. The angles, α and β, are the slope of the surface of the subregion with respect to x and y-axes respectively.

After imposing the variational condition obtained in Eq. (18) to all independent variables (p_{ij}, etc.) we obtain the following governing equations representing the equilibrium, compatibility, and boundary conditions for the RVE.

(a) Equilibrium equations, for $k=1,2,\ldots,N$ ($7N$ equations)

$$F_1^{(k)}=F_2^{(k)}=F_3^{(k)}=F_4^{(k)}=F_5^{(k)}=F_6^{(k)}=F_7^{(k)}=0\quad\text{for } k=1,2,\ldots,N \tag{20}$$

(b) Subregion compatibility equations, for $k=1,2,\ldots,N$: ($4N$ equations),

$$\chi_{33}^{(k)}=\chi_{34}^{(k)}=\chi_{43}^{(k)}=\chi_{53}^{(k)}=0 \tag{21}$$

where

$$\chi_{iL}^{(k)}=\eta_{iL}^{(k)}-E_{iL}^{(k)}-\hat{S}_{ijKL}^{(k)}p_{jK}^{(k)};$$

$$\hat{S}_{ijKL}^{(k)}=\int_{h_1^{(k)}}^{h_2^{(k)}}S_{ij}^{(k)}f_K^{(j)}f_L^{(i)}\,\mathrm{d}z \tag{22}$$

(c) Interface compatibility equations, for $k=1,2,\ldots,N-1$: ($12N-12$ equations),

Consider a perfectly bonded interface between the kth and lth subregions (yarns). Here the lth subregion is considered on top of the kth subregion (i.e., lth subregion is at a higher z-value than that of the kth subregion).

$$\chi_{i1}^{(l)} + \chi_{i2}^{(k)} = 0 \quad \text{for } i = 1, 2, \ldots, 6 \tag{23}$$

$$\chi_{12}^{(k)} + h_{2,x}^{(k)}\chi_{52}^{(k)} + \left(h_{2,x}^{(k)}\right)^2 \chi_{32}^{(k)} = 0 \tag{24}$$

$$\chi_{22}^{(k)} + h_{2,y}^{(k)}\chi_{42}^{(k)} + \left(h_{2,y}^{(k)}\right)^2 \chi_{32}^{(k)} = 0 \tag{25}$$

$$\chi_{62}^{(k)} + h_{2,x}^{(k)}\chi_{42}^{(k)} + h_{2,y}^{(k)}\chi_{52}^{(k)} + 2h_{2,x}^{(k)}h_{2,y}^{(k)}\chi_{32}^{(k)} = 0 \tag{26}$$

$$p_{52}^{(k)} - h_{2,x}^{(k)}p_{12}^{(k)} - h_{2,y}^{(k)}p_{62}^{(k)} - p_{51}^{(l)} + h_{2,x}^{(k)}p_{11}^{(l)} + h_{2,y}^{(k)}p_{61}^{(l)} = 0 \tag{27}$$

$$p_{42}^{(k)} - h_{2,x}^{(k)}p_{62}^{(k)} - h_{2,y}^{(k)}p_{22}^{(k)} - p_{41}^{(l)} + h_{2,x}^{(k)}p_{61}^{(l)} + h_{2,y}^{(k)}p_{21}^{(l)} = 0 \tag{28}$$

$$p_{32}^{(k)} - h_{2,x}^{(k)}p_{52}^{(k)} - h_{2,y}^{(k)}p_{42}^{(k)} - p_{31}^{(l)} + h_{2,x}^{(k)}p_{51}^{(l)} + h_{2,y}^{(k)}p_{41}^{(l)} = 0 \tag{29}$$

(d) Boundary conditions (12 equations)

1. Top surface of the RVE (six equations)

$$\chi_{12}^{(n)} + h_{2,x}^{(n)}\chi_{52}^{(n)} + \left(h_{2,x}^{(n)}\right)^2 \chi_{32}^{(n)} = 0 \tag{30}$$

$$\chi_{22}^{(n)} + h_{2,y}^{(n)}\chi_{42}^{(n)} + \left(h_{2,y}^{(n)}\right)^2 \chi_{32}^{(n)} = 0 \tag{31}$$

$$\chi_{62}^{(n)} + h_{2,x}^{(n)}\chi_{42}^{(n)} + h_{2,y}^{(n)}\chi_{52}^{(n)} + 2h_{2,x}^{(n)}h_{2,y}^{(n)}\chi_{32}^{(n)} = 0 \tag{32}$$

$$\chi_{52}^{(n)} + h_{2,x}^{(n)}\chi_{32}^{(n)} + \tilde{u}_2^{(n)} = 0 \tag{33a}$$

or

$$\cos\alpha_n \cos\beta_n p_{52}^{(n)} - \sin\alpha_n \cos\beta_n p_{12}^{(n)} - \cos\alpha_n \sin\beta_n p_{62}^{(n)} = \tilde{\tau}_{x2}^{(n)} \tag{33b}$$

$$\chi_{42}^{(n)} + h_{2,y}^{(n)}\chi_{32}^{(n)} + \tilde{v}_2^{(n)} = 0 \tag{34a}$$

or

$$\cos\alpha_n \cos\beta_n p_{42}^{(n)} - \sin\alpha_n \cos\beta_n p_{62}^{(n)} - \cos\alpha_n \sin\beta_n p_{22}^{(n)} = \tilde{\tau}_{y2}^{(n)} \tag{34b}$$

$$\chi_{32}^{(n)} + \tilde{w}_2^{(n)} = 0 \tag{35a}$$

or

$$\cos\alpha_n \cos\beta_n p_{32}^{(n)} - \sin\alpha_n \cos\beta_n p_{52}^{(n)} - \cos\alpha_n \sin\beta_n p_{42}^{(n)} = \tilde{\tau}_{z2}^{(n)} \tag{35b}$$

2. Bottom surface of the RVE (six equations)

$$\chi_{11}^{(m)} + h_{1,x}^{(m)}\chi_{51}^{(m)} + \left(h_{1,x}^{(m)}\right)^2\chi_{31}^{(m)} = 0 \tag{36}$$

$$\chi_{21}^{(m)} + h_{1,y}^{(m)}\chi_{41}^{(m)} + \left(h_{1,y}^{(m)}\right)^2\chi_{31}^{(m)} = 0 \tag{37}$$

$$\chi_{61}^{(m)} + h_{1,x}^{(m)}\chi_{41}^{(m)} + h_{1,y}^{(m)}\chi_{51}^{(m)} + 2h_{1,x}^{(m)}h_{1,y}^{(m)}\chi_{31}^{(m)} = 0 \tag{38}$$

$$\chi_{51}^{(m)} + h_{1,x}^{(m)}\chi_{31}^{(m)} - \tilde{u}_1^{(m)} = 0 \tag{39a}$$

or

$$\cos\alpha_m\cos\beta_m p_{51}^{(m)} - \sin\alpha_m\cos\beta_m p_{11}^{(m)} - \cos\alpha_m\sin\beta_m p_{61}^{(m)} = \tilde{\tau}_{x1}^{(m)} \tag{39b}$$

$$\chi_{41}^{(m)} + h_{1,y}^{(m)}\chi_{31}^{(m)} - \tilde{v}_1^{(m)} = 0 \tag{40a}$$

or

$$\cos\alpha_m\cos\beta_m p_{41}^{(m)} - \sin\alpha_m\cos\beta_m p_{61}^{(m)} - \cos\alpha_m\sin\beta_m p_{21}^{(m)} = \tilde{\tau}_{y1}^{(m)} \tag{40b}$$

$$\chi_{31}^{(m)} - \tilde{w}_1^{(m)} = 0 \tag{41a}$$

or

$$\cos\alpha_m\cos\beta_m p_{31}^{(m)} - \sin\alpha_m\cos\beta_m p_{51}^{(m)} - \cos\alpha_m\sin\beta_m p_{41}^{(m)} = \tilde{\tau}_{z1}^{(m)} \tag{41b}$$

The subscripts or superscripts m and n are associated with the bottom and top surfaces of the RVE, respectively. α and β are the angles of the slope of the subregion surface along the x and y directions, respectively. There are 29 unknown variables for each subregion (yarn or matrix region) in the model. For an N number of subregions, Eqs. (20)–(41a) and (41b) yield a set of $23N$ governing (or characteristic) equations. The other remaining $6N$ equations are the interface displacement continuity conditions $(u_1^{(l)} = u_2^{(k)}, \ldots, w_1^{(l)} = w_2^{(k)})$. There are possible two approaches (finite element or finite difference) may be taken to solve the above system of equations. A solution procedure for this system of equations is given in a following paper, Part-II (Sihn and Roy, 2000). The three-dimensional stress field of the RVE of the woven composites can then be calculated after solving the above system of equations.

Appendix A

Notations used in Eq. (14)

$$\chi_{iL}^{(k)} = \eta_{iL}^{(k)} - E_{iL}^{(k)} - \hat{S}_{ijKL}^{(k)}p_{jK}^{(k)}$$

where

$$\hat{S}_{ijKL}^{(k)} = \int_{h_1^{(k)}}^{h_2^{(k)}} S_{ij}^{(k)} f_K^{(j)} f_L^{(i)}\,\mathrm{d}z, \qquad E_{iL}^{(k)} = \int_{h_1^{(k)}}^{h_2^{(k)}} e_i^{(k)} f_L^{(i)}\,\mathrm{d}z,$$

and S_{ij} is the compliance matrix.

$$\eta_{11}^{(k)} = \left(h_2^{(k)} - h_1^{(k)}\right)\frac{\partial \bar{u}^{(k)}}{\partial x} + \frac{\partial\left(h_2^{(k)} - 2h_1^{(k)}\right)}{\partial x}\bar{u}^{(k)} - \frac{\partial h_2^{(k)}}{\partial x}u^{*(k)}$$

$$\eta_{12}^{(k)} = \left(h_2^{(k)} - h_1^{(k)}\right)\frac{\partial u^{*(k)}}{\partial x} + \frac{\partial\left(2h_2^{(k)} - h_1^{(k)}\right)}{\partial x}u^{*(k)} + \frac{\partial h_1^{(k)}}{\partial x}\bar{u}^{(k)}$$

$$\eta_{21}^{(k)} = \left(h_2^{(k)} - h_1^{(k)}\right)\frac{\partial \bar{v}^{(k)}}{\partial y} + \frac{\partial\left(h_2^{(k)} - 2h_1^{(k)}\right)}{\partial y}\bar{v}^{(k)} - \frac{\partial h_2^{(k)}}{\partial y}v^{*(k)}$$

$$\eta_{22}^{(k)} = \left(h_2^{(k)} - h_1^{(k)}\right)\frac{\partial v^{*(k)}}{\partial y} + \frac{\partial\left(2h_2^{(k)} - h_1^{(k)}\right)}{\partial y}v^{*(k)} + \frac{\partial h_1^{(k)}}{\partial y}\bar{v}^{(k)}$$

$$\eta_{31}^{(k)} = \bar{w}^{(k)} + w^{*(k)}, \quad \eta_{32}^{(k)} = \left(\bar{w}^{(k)} + w^{*(k)}\right), \quad \eta_{33}^{(k)} = \bar{w}^{(k)} - w^{*(k)}, \quad \eta_{34}^{(k)} = -6\hat{w}^{(k)} - \bar{w}^{(k)} - w^{*(k)}$$

$$\eta_{41}^{(k)} = \bar{v}^{(k)} + v^{*(k)} + \left(h_2^{(k)} - h_1^{(k)}\right)\frac{\partial \bar{w}^{(k)}}{\partial y} + \frac{\partial\left(h_2^{(k)} - 2h_1^{(k)}\right)}{\partial y}\bar{w}^{(k)} - \frac{\partial h_2^{(k)}}{\partial y}w^{*(k)}$$

$$\eta_{42}^{(k)} = -\bar{v}^{(k)} - v^{*(k)} + \left(h_2^{(k)} - h_1^{(k)}\right)\frac{\partial w^{*(k)}}{\partial y} + \frac{\partial\left(2h_2^{(k)} - h_1^{(k)}\right)}{\partial y}w^{*(k)} + \frac{\partial h_1^{(k)}}{\partial y}\bar{w}^{(k)}$$

$$\eta_{43}^{(k)} = \bar{v}^{(k)} - v^{*(k)} + \left(h_2^{(k)} - h_1^{(k)}\right)\frac{\partial \hat{w}^{(k)}}{\partial y} + 3\frac{\partial\left(h_2^{(k)} - h_1^{(k)}\right)}{\partial y}\hat{w}^{(k)} + \frac{\partial h_2^{(k)}}{\partial y}w^{*(k)} - \frac{\partial h_1^{(k)}}{\partial y}\bar{w}^{(k)}$$

$$\eta_{51}^{(k)} = \bar{u}^{(k)} + u^{*(k)} + \left(h_2^{(k)} - h_1^{(k)}\right)\frac{\partial \bar{w}^{(k)}}{\partial x} + \frac{\partial\left(h_2^{(k)} - 2h_1^{(k)}\right)}{\partial x}\bar{w}^{(k)} - \frac{\partial h_2^{(k)}}{\partial x}w^{*(k)}$$

$$\eta_{52}^{(k)} = -\bar{u}^{(k)} - u^{*(k)} + \left(h_2^{(k)} - h_1^{(k)}\right)\frac{\partial w^{*(k)}}{\partial x} + \frac{\partial\left(2h_2^{(k)} - h_1^{(k)}\right)}{\partial x}w^{*(k)} + \frac{\partial h_1^{(k)}}{\partial x}\bar{w}^{(k)}$$

$$\eta_{53}^{(k)} = \bar{u}^{(k)} - u^{*(k)} + \left(h_2^{(k)} - h_1^{(k)}\right)\frac{\partial \hat{w}^{(k)}}{\partial x} + 3\frac{\partial\left(h_2^{(k)} - h_1^{(k)}\right)}{\partial x}\hat{w}^{(k)} + \frac{\partial h_2^{(k)}}{\partial x}w^{*(k)} - \frac{\partial h_1^{(k)}}{\partial x}\bar{w}^{(k)}$$

$$\eta_{61}^{(k)} = \left(h_2^{(k)} - h_1^{(k)}\right)\left(\frac{\partial \bar{u}^{(k)}}{\partial y} + \frac{\partial \bar{v}^{(k)}}{\partial x}\right) + \frac{\partial\left(h_2^{(k)} - 2h_1^{(k)}\right)}{\partial x}\bar{v}^{(k)} + \frac{\partial\left(h_2^{(k)} - 2h_1^{(k)}\right)}{\partial y}\bar{u}^{(k)} - \frac{\partial h_2^{(k)}}{\partial x}v^{*(k)} - \frac{\partial h_2^{(k)}}{\partial y}u^{*(k)}$$

$$\eta_{62}^{(k)} = \left(h_2^{(k)} - h_1^{(k)}\right)\left(\frac{\partial u^{*(k)}}{\partial y} + \frac{\partial v^{*(k)}}{\partial x}\right) + \frac{\partial\left(2h_2^{(k)} - h_1^{(k)}\right)}{\partial x}v^{*(k)} + \frac{\partial\left(2h_2^{(k)} - h_1^{(k)}\right)}{\partial y}u^{*(k)} + \frac{\partial h_1^{(k)}}{\partial x}\bar{v}^{(k)} + \frac{\partial h_1^{(k)}}{\partial y}\bar{u}^{(k)}$$

$$\mu_{11}^{(k)} = \frac{\partial h_1^{(k)}}{\partial x}u_1^{(k)}, \quad \mu_{12}^{(k)} = -\frac{\partial h_2^{(k)}}{\partial x}u_2^{(k)}, \quad \mu_{21}^{(k)} = \frac{\partial h_1^{(k)}}{\partial y}v_1^{(k)}, \quad \mu_{22}^{(k)} = -\frac{\partial h_2^{(k)}}{\partial y}v_2^{(k)}$$

$$\mu_{31}^{(k)} = -w_1^{(k)}, \quad \mu_{32}^{(k)} = w_2^{(k)}, \quad \mu_{41}^{(k)} = \frac{\partial h_1^{(k)}}{\partial y} w_1^{(k)} - v_1^{(k)}, \quad \mu_{42}^{(k)} = -\frac{\partial h_2^{(k)}}{\partial y} w_2^{(k)} + v_2^{(k)}$$

$$\mu_{51}^{(k)} = \frac{\partial h_1^{(k)}}{\partial x} w_1^{(k)} - u_1^{(k)}, \qquad \mu_{52}^{(k)} = -\frac{\partial h_2^{(k)}}{\partial x} w_2^{(k)} + u_2^{(k)}$$

$$\mu_{61}^{(k)} = \frac{\partial h_1^{(k)}}{\partial y} u_1^{(k)} + \frac{\partial h_1^{(k)}}{\partial x} v_1^{(k)}, \qquad \mu_{62}^{(k)} = -\left(\frac{\partial h_2^{(k)}}{\partial y} u_2^{(k)} + \frac{\partial h_2^{(k)}}{\partial x} v_2^{(k)} \right)$$

$$F_1^{(k)} = \left(h_2^{(k)} - h_1^{(k)}\right) \left(\frac{\partial p_{11}^{(k)}}{\partial x} + \frac{\partial p_{61}^{(k)}}{\partial y} \right) + \left(p_{11}^{(k)} - p_{12}^{(k)}\right) \frac{\partial h_1^{(k)}}{\partial x} + \left(p_{61}^{(k)} - p_{62}^{(k)}\right) \frac{\partial h_1^{(k)}}{\partial y} - p_{51}^{(k)} + p_{52}^{(k)} - p_{53}^{(k)}$$

$$F_2^{(k)} = \left(h_2^{(k)} - h_1^{(k)}\right) \left(\frac{\partial p_{12}^{(k)}}{\partial x} + \frac{\partial p_{62}^{(k)}}{\partial y} \right) + \left(p_{11}^{(k)} - p_{12}^{(k)}\right) \frac{\partial h_2^{(k)}}{\partial x} + \left(p_{61}^{(k)} - p_{62}^{(k)}\right) \frac{\partial h_2^{(k)}}{\partial y} - p_{51}^{(k)} + p_{52}^{(k)} + p_{53}^{(k)}$$

$$F_3^{(k)} = \left(h_2^{(k)} - h_1^{(k)}\right) \left(\frac{\partial p_{61}^{(k)}}{\partial x} + \frac{\partial p_{21}^{(k)}}{\partial y} \right) + \left(p_{61}^{(k)} - p_{62}^{(k)}\right) \frac{\partial h_1^{(k)}}{\partial x} + \left(p_{21}^{(k)} - p_{22}^{(k)}\right) \frac{\partial h_1^{(k)}}{\partial y} - p_{41}^{(k)} + p_{42}^{(k)} - p_{43}^{(k)}$$

$$F_4^{(k)} = \left(h_2^{(k)} - h_1^{(k)}\right) \left(\frac{\partial p_{62}^{(k)}}{\partial x} + \frac{\partial p_{22}^{(k)}}{\partial y} \right) + \left(p_{61}^{(k)} - p_{62}^{(k)}\right) \frac{\partial h_2^{(k)}}{\partial x} + \left(p_{21}^{(k)} - p_{22}^{(k)}\right) \frac{\partial h_2^{(k)}}{\partial y} - p_{41}^{(k)} + p_{42}^{(k)} + p_{43}^{(k)}$$

$$F_5^{(k)} = \left(h_2^{(k)} - h_1^{(k)}\right) \left(\frac{\partial p_{51}^{(k)}}{\partial x} + \frac{\partial p_{41}^{(k)}}{\partial y} \right) + \left(p_{51}^{(k)} - p_{52}^{(k)} + p_{53}^{(k)}\right) \frac{\partial h_1^{(k)}}{\partial x} + \left(p_{41}^{(k)} - p_{42}^{(k)} + p_{43}^{(k)}\right) \frac{\partial h_1^{(k)}}{\partial y} - p_{31}^{(k)} + p_{32}^{(k)} - p_{33}^{(k)} + p_{34}^{(k)}$$

$$F_6^{(k)} = \left(h_2^{(k)} - h_1^{(k)}\right) \left(\frac{\partial p_{52}^{(k)}}{\partial x} + \frac{\partial p_{42}^{(k)}}{\partial y} \right) + \left(p_{51}^{(k)} - p_{52}^{(k)} - p_{53}^{(k)}\right) \frac{\partial h_2^{(k)}}{\partial x} + \left(p_{41}^{(k)} - p_{42}^{(k)} - p_{43}^{(k)}\right) \frac{\partial h_2^{(k)}}{\partial y} - p_{31}^{(k)} + p_{32}^{(k)} + p_{33}^{(k)} + p_{34}^{(k)}$$

$$F_7^{(k)} = \left(h_2^{(k)} - h_1^{(k)}\right) \left(\frac{\partial p_{53}^{(k)}}{\partial x} + \frac{\partial p_{43}^{(k)}}{\partial y} \right) - 2p_{53}^{(k)} \left(\frac{\partial h_2^{(k)}}{\partial x} - \frac{\partial h_1^{(k)}}{\partial x} \right) - 2p_{43}^{(k)} \left(\frac{\partial h_2^{(k)}}{\partial y} - \frac{\partial h_1^{(k)}}{\partial y} \right) + 6p_{34}^{(k)}$$

References

Chou, T., Ko, F.K., 1989. Textile Structural Composites, Elsevier, New York, USA (Chapter 7).

Harrison, P.E., Johnson, E.R., 1996. A mixed variational formulation for interlaminar stresses in thickness-tapered composite laminates. International Journal of Solids and Structures 33 (16), 2377–2399.

Karayaka, M., Kurath, P., 1994. Deformation and failure behavior of woven composite laminates. Journal of Engineering Materials and Technology 116 (2), 222–232.

Marrey, R.V., Sankar, B.V., 1995. Micromechanical Models for Textile Structural Composites, NASA CR 198229.

Naik, N.K., Ganesh, V.K., 1994. Failure behavior of plain weave fabric laminates under in-plane shear loading. Journal of Composites Technology and Research 16 (1), 3–20.

Pagano, N.J., 1978. Stress fields in composite laminates. International Journal of Solids and Structures 14, 385–400.

Reissner, E., 1950. On a variational theorem in elasticity. Journal of Mathematics and Physics 29, 90–95.

Roy, A.K., 1996. In situ damage observation and failure in model laminates containing planar yarn crimping of woven composites. Mechanics of Composite Materials and Structures 3, 101–117.

Roy, A.K., 1998. Comparison of in situ damage assessment in unbalanced fabric composite and model laminate of planar (one-directional) crimping. Journal of Composites Science and Technology 58, 1793–1801.

Sihn, S., Roy, A.K., 2000. Development of a three-dimensional mixed variational model for woven composites: part II – numerical solution and validation. International Journal of Solids and Structures 38, 5949–5962.

Whitcomb, J.D., 1991. Three-dimensional stress analysis of plain weave composites. In: O'Brien, T.K. (Ed.), Composite Materials: Fatigue and Fracture, vol. 3, ASTM STP 1110, American Society for Testing and Materials, Philadelphia, pp. 417–438.